Effect of explosive characteristics on the explosive welding of stainless steel to carbon steel in cylindrical configuration

R. Mendes, J.B. Ribeiro, A. Loureiro

PII: S0261-3069(13)00277-X
DOI: http://dx.doi.org/10.1016/j.matdes.2013.03.069
Reference: JMAD 5298

To appear in: *Materials and Design*

Received Date: 19 November 2012
Accepted Date: 22 March 2013

Please cite this article as: Mendes, R., Ribeiro, J.B., Loureiro, A., Effect of explosive characteristics on the explosive welding of stainless steel to carbon steel in cylindrical configuration, *Materials and Design* (2013), doi: http://dx.doi.org/10.1016/j.matdes.2013.03.069

Effect of explosive characteristics on the explosive welding of stainless steel to carbon steel in cylindrical configuration

R. Mendes[1], J.B. Ribeiro[1], A. Loureiro[2]

[1]ADAI - Assoc. for Dev. of Ind. Aerodynamics / LEDAP - Lab. Energetics and Detonics Department of Mechanical Engineering, University of Coimbra, Rua Luis Reis Santos, Polo II, 3030-788 Coimbra, Portugal

[2]CEMUC – Department of Mechanical Engineering, University of Coimbra, Rua Luis Reis Santos, 3030-788 Coimbra, Portugal

*Email address: ricardo.mendes@dem.uc.pt, tel. + (351) 239 790 700, fax. + (351) 239 790 771

Abstract

The aim of this research is to study the influence of explosive characteristics on the weld interfaces of stainless steel AISI 304L to low alloy steel 51CrV4 in a cylindrical configuration. The effect of ammonium nitrate-based emulsion, sensitized with different quantities and types of sensitizing agents (hollow glass microballoons or expanded polystyrene spheres) and Ammonium Nitrate Fuel Oil (ANFO) explosives on the interface characteristics is analyzed. Research showed that the type of explosive and the type and proportion of explosive sensitizers affect the main welding parameters, particularly collision point velocity. The morphology of the wavy weld interfaces, chiefly the amplitude and length of the waves, is affected both by the impact velocity and the type and particle size of the explosive sensitizers, and increases with particle size. All the weld interfaces, except welds done with ANFO, displayed localized melted and solidified regions, whose chemical composition resulted from the contribution of both flyer and base metal.

Keywords: explosive welding; emulsions explosive; low alloy and stainless steels.

1. Introduction

Explosive cladding or welding was first observed during World War I when soldiers noticed shrapnel casing bonding with steel or metallic surfaces. However, it was only in the 1940s that the first experiments were carried out by L. R. Carl in 1944. Later, in the 1950s, more thorough investigations were conducted by Rinehart and Pearson [1; 2] and in the 1960s by Philipchuck [3], Davenport and Duvall [4], Holtzman and Ruderhausen [5], Deribas [6], Zernov *et al.* [7], Bahrani and Crossland [8]. This is when the commercialization of explosive welded plates began at DuPont [5].

Explosive cladding/welding is usually considered a solid state process [9; 10] in which the detonation of a certain amount of an explosive composition accelerates one of the materials to be welded against the other in order to promote a high-velocity oblique collision (see Fig. 1) that causes severe, but localized, plastic flow at the interacting surfaces. The high speed of the collision, between 0.6 and 3 mm/μs, brings about pressures considerably greater than the strengths of any known material. This result in significant plastic deformation and the mixing of the surface layers of the materials to be bonded which can result in a linear or a wavy interface. Such extreme, localized, plastic deformations dissipate a considerable amount of kinetic energy of the colliding plates, and reduce considerably the amplitude of the reflecting tensile stress which tends to separates the plates. While the process is normally described as a cold technique, whereby no external heat is used to promote the bonding, localized high-temperatures are normally generated at the weld interface due the dynamics of the process. Temperatures of 700 ºC, at 1 mm from the surfaces, have been measured but it seems obvious that much higher temperatures (enough to melt, for example, molybdenum and niobium), are attained, at least for a few microseconds, at the interface [11]. The nature of the oblique collision is such that parts of this molten layer are ejected from the system as a monolithic jet or as a dispersed cloud of particles that breaks up the oxide and/or other contaminant layers that may exist at the surface of the material. The estimated cooling rate of the remaining molten material is approximately 10^5 K/s, due to contact with the relatively large bulk of the materials to be welded. Such high cooling rates lead to the formation of ultrafine, nanometer, grains with a random orientation.

Fig. 1-Schematic representation of the explosive welding process.

One of the greatest attributes of this technique is that it allows very large surface areas of dissimilar metals to be welded, which is not possible using conventional fusion welding. The welded metals remain in their wrought states, and no continuous cast structures are created; neither the microstructures, nor the mechanical and corrosive properties of the wrought parent components are altered; there are neither heat-affected zones nor continuous-melt bands exhibiting mixed chemistry; there is almost no diffusion of alloying elements between the components. Therefore, explosive welding is an effective joining method for virtually all combinations of metals. Its only limitation is the sufficient ductility (10%) and fracture toughness (30 J) of materials to undergo rapid deformation without fracture [12]. Explosive welding is mainly used for the production of laminated metals in the form of sheets, rods or pipes in order to improve their corrosion or wear resistance, thermal conductivity or even antifriction properties.

A notable characteristic of explosive welding is the formation of waves at the interface between the welded materials. In comparison with the other occurring interface geometries, flat/smooth or continuous melted, the wavy interface is the one producing the best welding characteristics [13-17]. For this reason, the mechanism of wave formation in explosive welding has been studied for years [18; 19]. Despite the efforts there is not a unique explanation for that phenomenon, and four different explanations can be found in the literature: a) the Jet Indentation Mechanisms, used by Abrahamson [20] and later by Bahrani *et al.* [21], in which the indentation action created by the jet (salient jet according to Abrahamson and re-entrant jet according to Bahrani *et al.*) is responsible for the creation of a hump ahead of the collision point. According to Bahrani *et al.* [21], the interaction between the hump and the re-entrant jet traps the ejected material and is responsible for the formation of vortices; b) the Flow Instability Mechanism: in this case the process of wave formation is considered a hydrodynamic phenomenon similar to what happens at the interface between two liquids with different horizontal velocities, which is known as Kelvin-Helmholz Instability. According to Hunt [22], the velocity discontinuity occurs between the parent plate and the re-entrant jet, and according to Robinson [23] between the parent plate and the salient jet. The instabilities that trigger the wave formation are either created as a result of wave interferences, as suggested by Ben-Artzy [18], or as a result of oscillations in the detonation wave process which are transmitted to the flyer plate and, through it, to the plate interface, as suggested by Plaksin *et al.* [24]; c) the Vortex Shedding Mechanism, according to several authors [19; 25] the waves are formed due to a vortex shedding mechanism similar to that responsible for the formation of the von Kármán Vortex Street which can be observed for the flow of a viscous

fluid after an obstacle; d) the Stress Wave Mechanism, proposed by El-Sobky and Blazynski [26]; In this case, the interface waves are the result of successive interference from rarefaction waves in both plates. Knowing which of these mechanisms better describes the process of wave formation has been a long-standing problem in the field of explosive welding. It may be, as Carton tried to demonstrate [19], that some of these mechanisms may occur at the same time and dominate over the others at different welding conditions.

Attempts to relate the explosive welding parameters to the characteristics of the interfacial waves began in Russia by Deribas and his team [27] at the end of the 1960s and beginning of the 1970s. Reid and Sherif [28] in the UK and Cowan *et al.* [29] in the US, predicted an increase in the wavelength of the interfacial waves as a function of the collision angle. Later, Jaramillo *et al.* [30], following the works of Cowan and Holtzman [31] and Salem and Al-Hassani [32], tried to link the wave characteristics to the ratio of the thicknesses of the base and flyer plates. Jaramillov found that the wavelength and wave amplitude increase with that value. He also found what he considered to be a considerable discrepancy between the experimental results of the wavelength and the calculations made using equations developed by Godunov *et al.* [27] assuming an hydrodynamic behaviour of the materials at the weld interface. Recently, Manikandan *et al.* [33] found a direct relation between the kinetic energy lost at the collision of the plates and the amplitude and length of the waves at the welding interface. The subject continues to merit the attention of several authors [18; 34-36]. Thanks to their work, and in accordance with older results, it has been found that the wavelength and the wave amplitude increase with the stand-off distance, the explosive load and the base plate thickness. Nevertheless, according to a model developed by Balasubramanian *et al.* [37] the amplitude and wavelength increases with the flyer plate thickness, in contrast to observations made by Cowan *et al.*[29], and Jaramillov *et al.* [30]. These discrepancies, as stated by Jaramillov *et al.* [30], suggest an insufficient understanding of the process of metal adhesion at high collision velocities.

The conditions that should be met in order to achieve good welds is called the weldability window or criteria. A weldability criterion based on the flyer plate velocity and flyer mechanical properties developed by Cowan *et al.* [29] is mentioned by Mousavi and Al-Hassani [38], and is considered to give poor results. Criteria based only on the collision point velocity, although allowing the development of empirical equations to establish the weldability limits, did not provide an overall picture of the process. At present, the most used and well-known weldability criterion is based on

the collision point velocity V_c, and on the collision angle β, as defined in Fig. 1. In the β- V_c space, the weldability window is defined by four lines or limits (vd. Fig. 2), the first theoretical explanation for which was offered by Wittman [39]. There are four conditions for the establishment of those limits. The first limit is linked to the formation of a jet at the collision point; the rightmost line of the weldability window is a consequence of this condition. To meet this condition, as stated by Walsh *at al.* [39], the collision point velocity should be smaller than the sound speed of the materials. This limiting value for collision point velocity is a weak function of the collision angle β, so instead of a straight vertical line the rightmost limit of the weldability window is a slightly concave left vertical line. The second limit is the formation of a wavy interface; the leftmost line of the weldability window is a consequence of this condition. Kuzmin and Lysac (vd. [40] cited in [10]) state that this line, which defines the transition collision velocity $V_{c,tr}$ (above which we end up with a wavy interface), is a function of the collision angle; so, it should not be a straight vertical line. However, most authors consider it a vertical line, and therefore independent of the collision angle. Cowan *et al.* [29] have even proposed the equation Eq. (1) for the determination of $V_{c,tr}$ (expressed in mm/μs) that appears as a function of the materials densities (ρ_p and ρ_f, for the density of the parent and flyer plate materials, expressed in kg/m^3), Vickers hardness $H_{V,p}$ and $H_{V,f}$ (expressed in N/mm^2) and a critical Reynolds Number (R_{cr}), that takes values between 8.0 and 13.0, for the asymmetric explosive welding configuration.

$$V_{c,tr} = \sqrt{\frac{2R_{cr}(H_{V,p} + H_{V,f})}{(\rho_p + \rho_f)}} \tag{1}$$

The third limit is the achievement of an impact velocity V_p, where by the impact pressure at the collision point exceeds the yield stress of the materials, in order to promote plastic deformation. The lower limit of the weldability window is a consequence of this condition. Deribas and Zakharenko, as mentioned by Zakharenko *el at.*[41], developed an equation for this limit (vd. Eq. 2), in which the minimum collision point velocity $V_{c,min}$, related to the impact velocity through the Eq. (5) is determined as a function of the material Vickers Hardness *Hv* [N/m^2], the material density ρ [kg/m^3], the collision angle β, and a constant *k1* of values between 0.6 (for clean surfaces), and 1.2 for imperfectly cleaned surfaces [42].

$$V_{c,min.} = \frac{k_1}{\beta}\sqrt{\frac{H_V}{\rho}} \tag{2}$$

The fourth and final condition is to keep the impact velocity below certain value, so that the dissipation of kinetic energy should not produce a continuous melted layer on the materials which are to be welded. The upper limit of the weldability window is related with this requirement. Wittman [43] has developed the equation (3) for maximum impact velocity which avoids the formation of a interfacial melted layer from which, using Eq. (5), it is possible to find a relationship between the collision angle and the collision point velocity (vd. Eq. 4) that defines the upper limit of the weldability window.

$$V_p = \frac{1}{N}\frac{(T_m C_0)^{1/2}}{V_c}\left(\frac{kC_pC_0}{\rho h}\right)^{1/4} \quad (3)$$

$$\sin\frac{\beta}{2} = \frac{1}{N}\frac{(T_m C_0)^{1/2}}{2V_c^2}\left(\frac{kC_pC_0}{\rho h}\right)^{1/4} \quad (4)$$

With all parameters referring to the flyer plate properties and where T_m is the melting temperature [^{o}C], k the thermal conductivity [erg/cm ^{o}C], C_p the thermal capacity [erg/g ^{o}C], ρ the material density in [g/cm^3], h the thickness [cm], C_0 the bulk sound speed [cm/s], and N a constant that for several metals takes the value of 0.11 [44], with β expressed in radians.

Fig. 2 – Generic weldability window with the definition of limits [14].

As the results from the previous description show, successful welding depends on V_c, V_p and β. However, once V_c and V_p are related through β we are left with only two independent variables. The angle of collision and the impact velocity are known to depend on parameters such as flyer plate thickness, stand-off distance (initial distance between the flyer and the parent or base plate), flyer geometry, explosive confinement (if any), the explosive to flyer mass ratio and the explosive energy. The collision point velocity is essentially determined by the properties of the explosive used to accelerate the flyer plate. So, once one of the limits of the weldability window determines that, for jet formation, the velocity of the collision point should be lower than the sound velocity, the use of high-explosives (such as plastic explosives, presenting detonation velocities of 6000-8000 m/s) is not possible in explosive welding.

Low velocity explosives are therefore needed for explosive welding. Moreover, fine tuning the welding conditions requires a proper control of its detonation velocity. Ammonium nitrated-based

emulsion explosives, which are based on a mixture of emulsion matrix with a sensitizer agent, are among the explosives which are suitable given this requirement. Several authors have shown [45]; [46] that the emulsion explosives can meet that requirement when their density is reduced. This is achieved by increasing the amount of sensitizers, such as hollow glass or polymer microballoons, in order to reduce the detonation velocity. Furthermore, emulsion explosives ensure low cost, water-resistance and a high level of safety and reliability. However, no studies on how the characteristics of the explosives and of the detonation process affect the weld quality are extant. The aim of this research is to study the influence of the explosive characteristics, in particular the type, amount and size of sensitizers on the interfaces features of a stainless steel to a low alloy steel weld in a cylindrical configuration. Moreover, the weldability window for the stainless steel to low alloy steel system was tested for the cylindrical configuration.

In this study, an ammonium nitrate-based emulsion, sensitized with different amounts and types of sensitizing agents, and Ammonium Nitrate Fuel Oil (ANFO) explosives were used to perform stainless steel AISI 304L tube to low alloy steel 51CrV4 (spring steel) rod welds.

2. Experimental procedure

2.1. Materials

Conventional explosive welding was conducted in cylindrical arrangement between TP 304L (ASTM A312) stainless steel tubes and 51CrV4 [47] spring steel rods using ammonium nitrate-based explosives. The chemical composition of steels can be seen in Table 1. The experimental setup is illustrated in Fig. 3.

Table 1 – Chemical composition of the materials to be welded.

Stainless steel tubes (18 mm diameter, 1.5 mm thick and 215 mm long) and rods (11.0 mm diameter and 210 mm long) were used. The internal surface of the tubes and the external surface of the rods were polished with abrasive paper of 500 grits, in order to reduce roughness of the surfaces. Rods were centered inside the tubes in order to create a uniform annular standoff distance of 2 mm. Concentric with both tube and rods a polyvinyl chloride tube (internal diameter 48 mm and length 290 mm) was used to contain the explosive. Tabs were used to maintain the distance between the components of the experimental apparatus. Four ionization probes,

positioned at fixed distances, were used in each setup to measure the detonation velocity. Five different ammonium nitrate-based emulsion explosives (ammonium nitrate (84%), water (10%) and oil plus emulsifier (6%)) were considered for this study. Three of those compositions were sensitized with different amounts (15%, 11% and 6%, w/w) of hollow glass microballons [HGMB], with an average diameter of 70 μm. The fourth and fifth were sensitized with different amounts (2% and 1.5% w/w) of expanded polystyrene spheres [EPS], with an average diameter of 1 mm. A sixth explosive composition, resulting from the mixture of ammonium nitrate (94%, w/w) and fuel oil (6%, w/w), known as ANFO, was also used. The weld experimental series and the density of the explosive used in each test are shown in Table 2.

Table 2 – Weld series and density of explosives used.

Fig. 3 – Schematic representation of the welding setup used in this study.

2.2. Detonation velocity measurements

Detonation velocity, defined as the velocity at which a detonation front propagates through a given explosive, is one of the most important detonation parameters. The detonation velocity is, by far, the easiest to measure. The simplest way to determine its value is to measure the time that the detonation wave [DW] takes to travel between two given points. To achieve this objective the experimental technique should be able to detect the DW arrival at those predefined points and measure the interval between successive events of that kind with a time resolution of several nanoseconds. In this case, we have taken advantage of the highly ionized detonation products at the detonation front to close, at each ionization probe, an open electrical circuit branch.

The resulting immediate changes in the circuit created by the closure of the branches at each probe are then recorded in an ultra-fast signal recorder, like a digital oscilloscope (in our case, a Tektronix DSA 602, with a time resolution of 1 ns). Fig. 4 shows a typical oscillogram obtained with this technique.

Fig. 4 - Typical example of a result used to determine the detonation velocity.

2.3. Microstructure and hardness

Specimens for microstructure analysis were extracted from the beginning and the end of welded coupons in planes parallel and perpendicular to the direction of propagation of the detonation wave. Specimens were ground and polished, according to ASTM E3-11, and electrolytic etched at 5 V for 45 s, using a solution of 15 g of oxalic acid in 150 ml of hydrogen peroxide. Microstructure examination was carried out using an optical microscope Zeiss Axiotec 100 HD and a Scanning Electron Microscope Philips XL30 with EDS. The elemental map distribution was achieved using an electron probe microanalyser Camebax SX50.

HV0.05 microhardness measurements, according to ASTM E384, were taken in longitudinal and transversal sections of the welds, in order to sample very small regions in the weld interfaces.

3. Results and discussion

3.1. Collision velocity and angle

During the welding process, the points A, B and C (see Fig. 1) form an isosceles triangle since the linear distance along the flyer and along the base plate, between the collision point at time zero (C) and the collision point at time *t* (when A hits B) must be the same. This means that the distance from C to A is equal to the distance from C to B. Once all the distances are directly related with velocities, it is possible to write the Eq. (5). In this very common case, when $\beta < 10^{o}$ is possible to simplify the Eq. (5) to the Eq. (6) with a minor error.

From the three parameters of Eq (5), the collision angle β, is the independent variable, the detonation velocity V_d *is* measured as described in section 2.2 and the impact velocity V_p is estimated from the Gurney Theory [48] adapted for converging configurations, as shown in Fig. 5, by equation (7) [49].

Fig. 5 – Schematics of converging configuration considered for impact velocity evaluation. *M* – Flyer tube; *C* – Explosive; *N*-External confinement.

$$\frac{1}{2}V_P = V_d.sin\left(\frac{\beta}{2}\right) \quad (5)$$

$$V_P = V_d.sin\,\beta \quad (6)$$

$$\frac{V_P}{\sqrt{2E}}=\left[A\left\{\frac{\left(\frac{M}{C}+\frac{\gamma+3}{6(\gamma+1)}\right)}{A}+A\left(\frac{N}{C}+\frac{3\gamma+1}{6(\gamma+1)}\right)-\frac{1}{3}\right\}\right]^{-1/2} \quad (7)$$

Where A is given by the Eq. (8)

$$A=\frac{\left[\frac{M}{C}+\left(\frac{M}{C}\right)(\gamma-1)+\frac{\gamma+2}{3(\gamma+1)}\right]}{\left(\frac{N}{C}+\frac{2\gamma+1}{3(\gamma+1)}\right)} \quad (8)$$

and γ by the Eq. (9)

$$\gamma=\frac{R_0}{R_i} \quad (9)$$

and where *M*, *C* and *N* are the mass per unit of length of the flyer tube, the explosive and the external confinement, respectively. In the equation (7) $\sqrt{2E}$, is the Gurney velocity, which according to Kennedy [48] is approximately 60% of the heat of explosion of the explosive composition.

Once the value of the impact velocity V_p given by the Eq. (7) corresponds to the terminal velocity, it is necessary to take into consideration its acceleration, in order to estimate the impact velocity at the point where the flyer tube collides with the inner cylinder, For this purpose, as suggested by Chou and Flis, [50], an exponential acceleration history, as given by the Eq. (10), was considered.

$$V_P(t)=V_{PGurney}\left[1-exp\left(-\frac{t-t_0}{\tau}\right)\right] \quad (10)$$

Where, $V_{pGurney}$ is the value of V_p given by the Eq. (7) and τ, the time constant, as given by the Eq. (11) as suggested by Chou *et al.* [51].

$$\tau=c_1\frac{M V_{PGurney}}{P_{CJ}}+c_2 \quad (11)$$

Where P_{CJ} is the Chapman-Jouguet detonation pressure and c_1 and c_2 are empirical constants.

Those constants were calibrated so that, as is typical for explosive metal flyer acceleration (see for example [52; 53]), after eight shock wave reflections its velocity reaches 80% of the Gurney Value (V_{pcal} = 0.8 $V_{pGurney}$). The time required by the flyer to achieve that velocity T_{Vpcal} was evaluated considering that, during the reflections, the shock wave propagates within the flyer at the longitudinal bulk sound speed of the steel C_b, (C_b = 4.496 mm/μs vd. [54], pag. 214), for a distance equivalent to eight times the flyer thickness and a time of 2.34 μs.

The calibration procedure is illustrated in Fig. 6 for the experiment "Weld 1". For this particular case, the time required to achieve 80% of the Gurney Velocity ($V_{ptarget}$ = 0.8 x 0.671 mm/μs) was $T_{Vptarget}$ = 2.34 μs. The empirical constants, c_1 and c_2 of the Eq. (10), were then chosen, so that flyer velocity matches that value at that time. Once calibrated, the constants c_1 and c_2, the application of the Eq. (7) and (9) and the use of a simple integration procedure of the velocity enable the results shown as open circles in the graph of Fig. 6. Given the initial gap between the flyer and the base rod of 2 mm, the collision velocity can be read from the same graph (now from the open diamond curve) for that travelling distance.

The measured detonation velocity V_d the calculated (according to the aforementioned procedure) impact velocity V_{pcal} and the collision angle β as well as the parameters used in the calculations, are shown in Table 3.

Fig. 6 – Procedure for calibrating of the constants c_1 and c_2 of Eq. (11) and evaluating the impact velocity.

Table 3 – Calculated values of V_d, V_{pcal} and β, as well as the parameters used for the calculations.

* ΔH is the heat of explosion. Values taken from Sanchidrián and Lopez[55].

3.2. Analysis of the welding conditions

As described in the introduction, a weldability window was built using the equations 1 to 3 and a limiting collision velocity equal to the lower bulk sound speed of the materials to be welded. In

this case, that value was found to be the one for stainless steel 304 L (4496 m/s [54]). The values used in the calculations are shown in Table 4, and the weldability window in Fig. 7. The conditions used in each of the welds are also plotted on that graph. As seen in that Figure, five of the six performed welds are slightly over the upper weldability limit. According to the literature, (see Fig. 2), those welds may present excessive melting. It is also possible to observe (see also Table 3) that, despite sharing the same basic energetic material (ammonium nitrate), it is the nature of the explosive composition, rather than its density, that mainly determines one of the welding parameters - the collision point velocity. In fact, although the explosives used in welds 1 and 6 present similar densities (0.774 and 0.760 g/cm^3, respectively), they show quite different collision point velocities (3667 and 2370m/s, respectively).

Table 4 – Values of the parameters of equations (1) to (3) used for the calculation of the weldability window. All values taken from references [55; 56] unless stated otherwise.

*In Eq. (2) the hardness of the base plate is expressed in [N/m^2]. **In the Eq. (3) the density of the flyer plate is expressed in [g/cm^3]. ***[54].

Fig. 7 – Weldability window for the stainless steel carbon steel combination and experimental conditions verified for the performed experiments.

3.3. Morphology of the outer surface of the welded samples

Fig. 8 shows the surface appearance of four of the welded samples. Figs 8a and 8b illustrate welds made using explosive sensitized with 15% (weld 1) and 8% (weld 3) of HGMB, respectively. The images show that on one hand weld 3, carried out with a higher collision point velocity and a smaller amount of HGMB, has a better surface appearance than weld 1, performed with lower V_c and a higher proportion of HGMB. On the other hand, weld 4 (explosive sensitized with EPS (2 % w/w) and a V_c higher than that of weld 6) shows much greater surface roughness, as can be seen from the comparison of Figs 8c and 8d. Weld 5 (explosive sensitized with 1.5% of EPS) displayed a surface appearance (not shown) similar to weld 4, with significant roughness, whilst weld 2 (explosive sensitized with 11% of HGMB) has an intermediate surface appearance (not shown) between weld 1 and weld 3.

These results show that the morphology of the outer surface of the welds is more a result of the type of sensitizing agent (HGMB or EPS) added to the emulsion matrix than of the explosive's density or collision point velocity. It seems that the superficial appearance of the stainless steel flyer is affected by some instability in the propagation of the detonation wave, induced by the sensitizer added to the explosive matrix, in this case HGMB or EPS. This disturbance appears to increase with the increase in diameter of the spheres of the sensitizer additive. The diameter of the polystyrene spheres (1 mm) is much higher than that of HGMB (70 μm), as previously mentioned. The surface appearance of each specimen described above is similar around the perimeter and along the length. Preliminary tests proved that the concentricity of the tube and rod is essential to obtain this result.

Fig. 8 – Surface appearance of the welded samples: a) Weld 1; b) Weld 3; c) Weld4; d) Weld 6.

3.4. Morphology of the weld interfaces

All the welds displayed wavy interfaces, with small melted regions coloured dark, as shown in Fig. 9. These melted regions may be incipient or even absent in weld 6, which used ANFO.

Fig. 9 – Morphology of the interface between carbon steel and stainless steel: a) weld 1; b) weld 2; c) weld 3; d) weld 4; e) weld 5 and f) weld 6. Definition of the amplitude (A) and wave length (λ).

The area of the melted regions varies with the type of sensitizer and also with the collision point velocity. For the welds using HGMB, the area of the melted regions increases as V_c increases (see Figs 9a to 9c). For weld 3, melted zones of successive waves are even connected, as illustrated in Fig. 9c. Welds performed with explosive containing EPS show large melted areas at the top and base of the waves (see Figs 9d and 9e). In addition, those melted area show voids that occur as the result of shrinkage during solidification, increasing their size as the volume of melted metal increases. Weld 6, performed with ANFO, and presenting the highest impact velocity (see table 3) shows waves identical to the weld carried out with the explosive sensitized with the highest amount of HGMB, but has very small melted areas, and even an absence of fusion, as illustrated in Fig. 9f. These results suggest that the morphology of the weld interfaces is affected not only by impact velocity, but also by the nature of the sensitizer added to the explosive. The

characterization of wave geometry was done in a simplified manner using the amplitude *A* and wavelength λ, as illustrated in Fig. 9a.

The effect of impact velocity on the amplitude and length of the waves at the weld interfaces is illustrated in Fig. 10.

Fig. 10 – Effect of impact velocity on the amplitude of waves at the weld interfaces.

Fig. 10 shows that welds done using explosive sensitized with HGMB result in increasing amplitude of the waves with increasing impact velocity, though wavelength displayed only a modest increase. The welds performed with explosive sensitized with EPS showed the same trend. However, these increasing rates are much higher for the welds performed with explosive sensitized with EPS than for the explosive sensitized with HGMB. In addition, the values of the amplitude and wavelength are themselves greater for the welds performed with the explosive sensitized with EPS than for the welds performed with explosive sensitized with HGMS.

The increase in wavelength and amplitude with the explosive load was also observed by Kahraman *et al.* [57] in welds between aluminum and titanium plates. According to Manikandan *et al.* [33], it is reasonable to link the loss of kinetic energy with the wavelength and wave amplitude, which is an essential requirement for inducing plastic flow for welding. Manikandan *et al.* [33] showed a consistent increase of the wavelength and amplitude of the interfacial waves with the loss of kinetic energy in titanium to stainless steel welds. As stated by Hokamoto *et al.* [58], once the loss of kinetic energy at the welding interface is a function of the impact velocity and of the mass of the colliding plates per unit of area it can be said that, for each kind of sensitizing agent, the results obtained are in accordance with the results of Manikandan *et al.* [33]. Zamani and Liaghat [42] also reported an increase in the length and amplitude of the waves at the interface with the increase of explosive loads for the welding of stainless steel to carbon steel coaxial pipes. However, none of the authors mention the effect of the nature of the explosive.

The effect of the collision angle on the morphology of the waves at the weld interfaces is illustrated in Fig. 11. The wave amplitude decreases as the collision angle increases in welds performed with explosive sensitized with HGMB, as opposed to welds done with explosive sensitized with EPS. However, weld 6, the one with the highest collision angle, displayed a low wave amplitude, similar to that of weld 3. The wavelength is not significantly affected by the collision angle for welds performed with explosive sensitized with HGMB: in fact, although it was

performed with the highest collision angle, weld 6 presents a wavelength similar to welds 1 to 3. Welds 4 and 5 (explosive sensitized with EPS) displayed the longest wavelength, regardless of the collision angle.

These results show that the variation of wave amplitude and length is much more a function of the explosive type than of the collision angle or impact velocity. Most of the previous attempts to link the welding parameters with the wave amplitude and length did not consider the influence of the explosive type. The most current parameters correlating with wave amplitude and length were the collision angle and the flyer and base plate thicknesses; amplitude and wave length increase with both parameters [30; 37].

However, Plaksin *et al.* [24] stated that the Kelvin-Helmoltz instabilities, which are nowadays accepted as one of the most likely mechanisms of the wave formation, are triggered by the flyer plate instabilities which, in turn, are a consequence of the oscillatory nature of the propagation of the detonation wave.

Fig. 11 – Effect of collision angle β on the amplitude (a) and wavelength (b) at the weld interface.

Those oscillations, related with the periodic variation of values of the local detonation velocity [24; 59], are much greater for the emulsion explosives sensitized with EPS than for those sensitized with HGMB. The much greater roughness of the external surface of the flyer tube for the welds performed with the explosives sensitized with EPS, when compared with the welds performed with explosive sensitized with HGMB, is an evidence of that difference. The erosion figures on the surface of metallic materials in contact with detonating explosive compositions are directly related with the spatial dimension of the detonation oscillations [60]. The deeper and further apart the surface dents are, the greater the oscillations in the detonation process. In accordance with what was observed, greater oscillations during the propagation of the detonation wave are believed to induce greater oscillations in the flight velocity of the flyer plate and in turn, larger interfacial waves.

Although the results do not show a clear variation of the wave size with the collision angle for each kind of explosive, they suggest that the size of the interfacial waves increases with the impact velocity. Higher impact velocities are expected to result in conditions at the collision interface closer to the hydrodynamic state, and thus more suitable for the “actuation” of the Kelvin-Helmoltz instabilities, and the formation of bigger waves.

3.5. Hardness at the interface

A substantial increase in hardness was observed at the interface of the welds, both on the sides of the stainless steel and the low alloy steel, as illustrated in Fig. 12. On the low alloy steel side, the hardness increases from 220 to 300 HV0.05 at the interface, and extends over a width of a few mm. On the stainless steel side, the hardness rises from 165 HV0.05 (the hardness of the base material shown by a dotted line in the Fig. 12) to values between 300 and 450 HV0.05, with the highest near the interface and decreasing with distance from it, as illustrated in Fig. 12. This increase in hardness is consistent with the large plastic deformation experienced by the flyer during the impact. In Fig. 9, it is noticeable that deformation lines parallel to the weld interface are present in the stainless steel, caused by strong plastic deformation of the flyer during impact against the base rod. The deformation is so marked that micro-cracks occur in the flyer. Such marked plastic deformation should alter the mechanical properties of the flyer, particularly its hardness. Kahraman *et al.* [61] observed similar plastic deformation in oblique explosion welding between titanium and stainless steel, with the grains close to the interface, elongated and oriented parallel to the detonation direction. In order to verify that hypothesis, hardness measurements were carried out on the most plastically deformed zone of the AISI 304 stainless steel tensile specimens tested up to rupture. The values measured reached 320 HV0.5, which are close to the minimum values measured on the stainless steel flyer tube. However, it was not possible to establish any correlation between the impact velocity and the hardness achieved in stainless steel, because of the gradient of hardness observed. A similar explanation was given by Kaçar *et al*. [12; 62] and Durgutlu *et al.* [63] for the hardness increase in stainless steel flyers.

Fig. 12 – Microhardness profiles in the cross section of the welds. CS – carbon steel; SS – stainless steel. Base materials hardness is indicated by slash-dot lines.

In the regions close to the weld interface where vortices occurred, hardness values measured were significantly above those mentioned in Fig. 12. Fig. 13 illustrates an example of a line of hardness measurements on weld 5, which shows that, in the melted and solidified zone at the base of a wave, the hardness indentations are much smaller than in carbon steel or stainless steel. Hardness values of approximately 700 HV0.05 were measured in all welds in which there was significant formation of melted and solidified areas. According to the equations of Yurioka *et al.* [64], these values of hardness correspond to a martensitic structure containing 0.49% C, which is

the carbon content of the carbon steel analyzed. However, the hardness within the melted regions is not uniform, as illustrated by the variation in the size indentation. This suggests variations in chemical composition inside melted region.

Fig. 13 – Hardness variation in a melted and solidified region of weld 4.

3.6. Analysis of melted zones

As shown, for all the welds, except ANFO, the crest and the base of the interfacial waves show the formation of melted zones with a high degree of hardness. The formation of these local melted areas results from the dissipation of kinetic energy of the impacting materials in the form of heat (Crossland [65] and Hokomato *et al.* [58]), and takes place according to the mechanism described by Bahrani *et al.* [21]. The formation of these zones is expected to be created with material from both the flyer and the base plates: stainless and carbon steels, respectively, although those contributions may not be uniform, as suggested by the variation in hardness measurements mentioned above. Fig. 14 shows the qualitative elemental distribution in the crest of a wave in weld 5. The area studied was 50 μm by 50 μm in order to include part of a melted region. The elements analyzed were those present in varying quantities in the carbon and stainless steels used in the study, such as iron, silicon, nickel and chromium.

The crest of the wave is located at the top right of the images and the molten zone at the bottom right, while the stainless steel is on the left side. The image of the elemental distribution of iron shows that the content of this element in the molten zone is higher than that of stainless steel, but lower than that of carbon steel according to the colour scale shown at the bottom of the Fig. 14. Since silicon, nickel and chromium appear in greater quantities in the melted and solidified region than in the carbon steel, but in lower values than in stainless steel, it can be stated that both materials have contributed to the formation of the melted and solidified area.

Fig. 14 – Elemental mapping in the crest and in the molten zone of a wave of the weld 5.

Fig. 15 – SEM image of the melted zone in the crest of a wave of a weld 5.

The image of the melted zone, which contains shrinkage holes of a wave of the weld 5, is illustrated in Fig. 15. The analysis of chemical composition at different points (1 and 2) within the

melted area, using energy dispersive X-ray spectroscopy, showed small differences in chemical composition, with the chromium varying between 9.74% and 7.19% wt and nickel between 4.49% and 3.84% wt. These results are consistent with the observations of Kaçar *and* Acarer [12] in welds of duplex stainless steel to carbon steel, where the molten zones resulted from the melting and mixing of both the flyer and the base material. These compositional differences are understandable, assuming that the heating and cooling rates experienced in the area are very high, and do not allow for complete mixing of the molten metal. In fact, according to Crossland [65] cooling rates about 10^5-10^7 K/s can be reached during solidification. Song *et al.* [66] also observed strong gradients in the chemical composition inside the molten regions in titanium to steel cladding.

4. Conclusions

The explosive welding of stainless steel AISI 304 to low alloy 51CrV4 steel in a cylindrical configuration was studied. A weldability window was determined for the experimental conditions used. The following conclusions can be drawn:

- The final appearance and roughness of the external surface of the flyer is greatly affected by the amount and nature of the sensitizing agent of the emulsion explosive.
- All the welds exhibited wavy interface morphology. Pockets of melted and solidified material could be found for the welds performed in conditions outside the weldability window, while for the welds within the window the melted regions are absent or insignificant.
- Interfacial wave amplitude and length were shown to be, for each kind of explosive/sensitizing agent, a function of the impact velocity.
- No relation was established between wave length and amplitude and collision angle.
- The wavelength and amplitude were much more affected by the type and size of explosive/sensitizing agent than by any other process parameter.
- The emulsion explosive sensitized with EPS exhibited the highest values for wave length and amplitude at the weld interface.
- Significant hardening was observed at the interface of both materials, due to severe plastic deformation suffered during the wave formation.
- High hardness values, typical of high carbon/high alloy martensite microstructure, were found at the melted and solidified zones of the interface.

- Those melted and solidified zones displayed shrinkage holes, as well as chemical compositions which are a result of the contributions of both tube and rod compositions.

Acknowledgements

This research is sponsored by FEDER through the program COMPETE – Programa Operacional Factores de Competitividade – and nationally through FCT – Fundação para a Ciência e a Tecnologia – under the project PEst-C/EME/UI0285/2011

The authors thank the MSc students in Mechanical Engineering Hugo Santos and João Pedro Carvalho for having carried out part of the experimental work presented in the article.

References

[1] Rinehart, J. and Pearson, J. . 1954. *Behavior of metals under impulsive loads*. Cleveland, Ohio: Aerican Society for Metals.

[2] Rinehart, John S., and John Pearson. 1963. *Explosive Working of Metals*. Edited by P. P. book. New York: Macmillan.

[3] Philipchuk. 1965. *Explosive Welding Statuts - 1965*. Proceedings of the A.S.T.M.E. Creative Manufacturing Seminar, Paper SP 65-100.

[4] Davenport, D. E., and Duvall. G. E. 1961. Explosive Welding. In *Advanced high energy rate forming : book II--explosive, electro-hydraulic, electro-magnetic, pneumatic-mechanical; Technical papers presented at the ASTME Creative Manufacturing Seminars*, SP 60-161.

[5] Holtzman, A. H., and C. G. Ruderhausen. 1962. Recent Advances in Metal Working with Explosives. *Sheet Metal Industries* 39:399.

[6] Deribas, A. A., V. M. Kudinov, F. I. Matveenkov, and V. A. Simonov. 1967. Explosive welding. *Combustion, Explosion, and Shock Waves* 3 (1):69-72.

[7] Zernow, L., I Liberman, and W. L. Kincheloe. 1961. *Explosive Welding, Compaction, Joining and Perforation*. Proceedings of the A.S.T.M.E. Creative Manufacturing Seminars, SP 60-141.

[8] Bahrani, A. S., and B. Crossland. 1964. Explosive Welding and Cladding: An introductory Survey and Preliminary Results. *Proceedings of Institute of Mechanical Engineers* 179 (7):264.

[9] Fehim, Findik. 2011. Recent developments in explosive welding. *Materials & Design* 32 (3):1081-1093.

[10] Lysak, V. I., and S. V. Kuzmin. 2012. Lower boundary in metal explosive welding. Evolution of ideas. *Journal of Materials Processing Technology* 212 (1):150-156.

[11] Ryabov, V.R., L.D. Dobrushin, and Jung-Gi Moon. 2003. *Welding of Bimetals: Welding and Allied Processes*. Kiev: E.O. Paton Electric Welding Institute.

[12] Kacar, R., and M. Acarer. 2003. Microstructure-property relationship in explosively welded duplex stainless steel-steel. *Materials Science and Engineering: A* 363 (1):290-296.

[13] Acarer, M., B. Gülenç, and F. Findik. 2004. The influence of some factors on steel/steel bonding quality on there characteristics of explosive welding joints. *Journal of Materials Science* V39 (21):6457-6466.

[14] El-Sobky, H. 1983. Mechanics of explosive welding. In *Explosive Welding Forming and Compaction*, 189-217, edited by T. Z. Blazynski. London: Applied Science Publishers.

[15] Vaidyanathan, P. V., and A. R. Ramanathan. 1992. Design for quality explosive welding. *Journal of Materials Processing Technology* 32 (1â€“2):439-448.
[16] Wronka, Bogumil. 2011. Testing of explosive welding and welded joints. Wavy character of the process and joint quality. *International Journal of Impact Engineering* 38 (5):309-313.
[17] Wylie, H. K. , P. E. G. Williams, and B. Crossland. 1971. *Futher experimental investigation of explosive welding parameters*. Proceedings of the 3rd International Conference of the Center for High Energy Rate Forming, 1.3.1-1.3.43, at University of Denver, Denver, Colorado.
[18] Ben-Artzy, A., A. Stern, N. Frage, V. Shribman, and O. Sadot. 2010. Wave formation mechanism in magnetic pulse welding. *International Journal of Impact Engineering* 37 (4):397-404.
[19] Carton, E. P. 2004. Wave Forming Mechanisms in Explosive Welding. In *Materials Science Forum 465-466*, 219-224, edited by 10.4028/www.scientific.net/MSF.465-466.219: Trans Tech Publications.
[20] Abrahamson, G. R. 1961. Permanente periodic surface deformation due to a travelling jet. *J. Appl. Mech.* 83:519-528.
[21] Bahrani, A. S., T. J. Black, and B. Crossland. 1967. The Mechanics of Wave Formation in Explosive Welding. *Proceedings of the Royal Society of London. Series A. Mathematical and Physical Sciences* 296 (1445):123-136.
[22] Hunt, J. N. 1968. Wave formation in explosive welding. *Philosophical Magazine* 17 (148):669-680.
[23] Robinson, J. L. 1975. Mechanics of wave formation in impact welding. *Philosophical Magazine* 31 (28):587-597.
[24] Plaksin, I., J. Campos, J. Ribeiro, R. Mendes, J. Direito, D. Braga, and R. Pruemmer. 2003. Novelties in physics of explosive welding and powder compaction. *J. Phys. IV France* 110 797-802.
[25] Reid, S. R. 1974. A discussion of the mechanism of interface wave generation in explosive welding. *International Journal of Mechanical Sciences* 16:399.
[26] El-Sobky, H., and T. Z. Blazynski. 1975. *Experimental investigation of the mechanisms of explosive welding by means of a liquid analogue*. Proceedings of the Proceedings of the Fifth international Conference on High Energy Rate Fabrication, 1-21, at Denver, Colorado.
[27] Godunov, S. K., A. A. Deribas, and N. S. Kozin. 1971. Wave formation in explosive welding. *Journal of Applied Mechanics and Technical Physics* 12 (3):398-406.
[28] Reid, S. R., and N. H. S. Sherif. 1976. Prediction of the wavelength of interface waves in symmetric explosive welding. *Journal of Mechanical Engineering Science* 18 (2):87-94.
[29] Cowan, G., O. Bergmann, and A. Holtzman. 1971. Mechanism of bond zone wave formation in explosion-clad metals. *Metallurgical and Materials Transactions B* 2 (11):3145-3155.
[30] Jaramillov, D., O. T. Inal, and A. Szecket. 1987. Effect of base plate thickness on wave size and wave morphology in explosively welded couples. *Journal of Materials Science* 22 (9):3143-3147.
[31] Cowan, George R., and Arnold H. Holtzman. 1963. Flow Configurations in Colliding Plates: Explosive Bonding. *Journal of Applied Physics* 34 (4):928-939.
[32] Salem, S. A. L, and S. T. S. Al-Hassani. 1981. Interfacial wave generation in explosive welding of multilaminates In *Shock Waves and High Strain Rate Phenomena in Metals: Cocepts and Applications. Proceedings of the International Conference on Metallurgical Effects of High-Strain-Rate Deformation and Fabrication* 1003-1018, edited by M. A. Meyers and L. E. Murr. New York: Plenum Press.

[33] Manikandan, P., K. Hokamoto, M. Fujita, K. Raghukandan, and R. Tomoshige. 2008. Control of energetic conditions by employing interlayer of different thickness for explosive welding of titanium/304 stainless steel. *Journal of Materials Processing Technology* 195 (1â€“3):232-240.

[34] Acarer, Mustafa, BehÃ§et GÃ¼lenÃ§, and Fehim Findik. 2003. Investigation of explosive welding parameters and their effects on microhardness and shear strength. *Materials & Design* 24 (8):659-664.

[35] Durgutlu, Ahmet, Hasan Okuyucu, and Behcet Gulenc. 2008. Investigation of effect of the stand-off distance on interface characteristics of explosively welded copper and stainless steel. *Materials & Design* 29 (7):1480-1484.

[36] Lysak, V. I., and S. V. Kuzmin. 2003. *Explosive welding of metal layered composite materials*. Edited by E. O. P. E. W. I. o. t. N. A. o. S. o. Ukraine. Kiev.

[37] Balasubramanian, V., M. Rathinasabapathi, and K. Raghukandan. 1997. Modelling of process parameters in explosive cladding of mildsteel and aluminium. *Journal of Materials Processing Technology* 63 (1â€“3):83-88.

[38] Akbari Mousavi, A. A., and S. T. S. Al-Hassani. 2005. Numerical and experimental studies of the mechanism of the wavy interface formations in explosive/impact welding. *Journal of the Mechanics and Physics of Solids* 53 (11):2501-2528.

[39] Walsh, J. M., R. G. Shreffler, and F. J. Willig. 1953. Limiting Conditions for Jet Formation in High Velocity Collisions. *Journal of Applied Physics* 24 (3):349-359.

[40] Kuzmin, S. V., and V. I. Lysak. 1991. Main regularities of transfer to waveless modes of joint formation in explosive welding. In *Explosive Welding and Properties of Welded Joints. Inter-Departmental TransactionVolgograd Polytechnic Institute,* , 29-38. Volgograd.

[41] Zakharenko, I., and B. Zlobin. 1983. Effect of the hardness of welded materials on the position of the lower limit of explosive welding. *Combustion, Explosion, and Shock Waves* 19 (5):689-692.

[42] Zamani, E., and G. H. Liaghat. 2012. Explosive welding of stainless steel-carbon steel coaxial pipes. *Journal of Materials Science* 47 (2):685-695.

[43] Wittman, R. H. 1973. *The influence of collision parameters on the strength and microstructure of an explosion welded aluminum alloy*. Proceedings of the Second International Symposium on the Use of Explosive Energy in Manufacturing, 153-168, at Marianskie Lazni, Czechoslovakia

[44] de Rosset, William S. 2006. Analysis of Explosive Bonding Parameters. *Materials and Manufacturing Processes* 21 (6):634-638.

[45] Sil'vestrov, V., and A. Plastinin. 2009. Investigation of low detonation velocity emulsion explosives. *Combustion, Explosion, and Shock Waves* 45 (5):618-626.

[46] Mendes, Ricardo, Jose B. Ribeiro, I. Plaksin, and Jose Campos. 2012. Non ideal detonation of emulsion explosives mixed with metal particles. *AIP Conference Proceedings* 1426 (1):267-270.

[47] *EN 10089:2002, Hot rolled steels for quenched and tempered springs - Technical delivery conditions*. European Committee for Standardization. 2002.

[48] Kennedy, James E., Jonas A. Zukas, and William P. Walters. 1998. The Gurney Model of Explosive Output for Driving Metal Explosive Effects and Applications, 221-257, edited by L. Davison and Y. Hori: Springer New York.

[49] Hirsch, E. 1986. Improved Gurney Formulas for Exploding Cylinders and Spheres using "Hard Core" Approximation. *Propellants, Explosives, Pyrotechnics* 11 (3):81-84.

[50] Chou, P. C., and W. J. Flis. 1986. Recent Developments in Shaped Charge Technology. *Propellants, Explosives, Pyrotechnics* 11 (4):99-114.

[51] Chou, P. C., J. Carleone, W. J. Flis, R. D. Ciccarelli, and E. Hirsch. 1983. Improved formulas for velocity, acceleration, and projection angle of explosively driven liners. *Propellants, Explosives, Pyrotechnics* 8 (6):175-183.

[52] Tan, Duowang, Chengwei Sun, and Yanping Wang. 2003. Acceleration and Viscoplastic Deformation of Spherical and Cylindrical Casings under Explosive Loading. *Propellants, Explosives, Pyrotechnics* 28 (1):43-47.

[53] Tarver, C. M., R. D. Breithaupt, and J. W. Kury. 1997. Detonation waves in pentaerythritol tetranitrate. *Journal of Applied Physics* 81 (11):7193-7202.

[54] Marsh, S. P., ed. 1980. LASL Shock Hugoniot Data, *Los Alamos series on dynamic material properties*. Berkley: University of California Press.

[55] José A. Sanchidrián, Lina M López. 2006. Calculation of the Energy of Explosives with a Partial Reaction Model. Comparison with Cylinder Test Data. *Propellants, Explosives, Pyrotechnics* 31 (1):25-32.

[56] Steel, A K. 2012. *304/304L product data sheet* 2012 [cited March 2012].

[57] Kahraman, Nizamettin, Behcet Gulenc, and Fehim Findik. 2007. Corrosion and mechanical-microstructural aspects of dissimilar joints of Tiâ€“6Alâ€“4V and Al plates. *International Journal of Impact Engineering* 34 (8):1423-1432.

[58] Hokamoto, K., A. Chiba, M. Fujita, and T. Izuma. 1995. Single-shot explosive welding technique for the fabrication of multilayered metal base composites: effect of welding parameters leading to optimum bonding condition. *Composites Engineering* 5 (8):1069-1079.

[59] Mendes, R., J. Ribeiro, I. Plaksin, and J. Campos. 2007. Features of the detonation behaviour of the emulsion explosives. In *Proceedings of the 10th International Seminar NTREM - NEW TRENDS IN RESEARCH OF ENERGETIC MATERIALS*, 792-801. Pardubice: UNIVERSITY OF PARDUBICE, Faculty of Chemical Technology, Institute of Energetic Materials.

[60] Plaksin, I., J. Campos, J. Direito, R. Mendes, J. Ribeiro, J. Gois, P. Simoes, L. Pedroso, A. Portugal, J. Kennedy, and S. Coffey. 2005. Synergetic phenomena in detonation of solid heterogeneous explosives - Control of oscillations and dissipative structures in detonation flow. In *2005 International Conference on Physics and Control*, 33-40, edited by A. L. Fradkov and A. N. Churilov.

[61] Kahraman, Nizamettin, BehÃ§et GÃ¼lenÃ§, and Fehim Findik. 2005. Joining of titanium/stainless steel by explosive welding and effect on interface. *Journal of Materials Processing Technology* 169 (2):127-133.

[62] Kacar, Ramazan, and Mustafa Acarer. 2004. An investigation on the explosive cladding of 316L stainless steel-din-P355GH steel. *Journal of Materials Processing Technology* 152 (1):91-96.

[63] Durgutlu, Ahmet, BehÃ§et GÃ¼lenÃ§, and Fehim Findik. 2005. Examination of copper/stainless steel joints formed by explosive welding. *Materials & Design* 26 (6):497-507.

[64] Yurioka, N., Okumura M., Kasuya T., and Cotton H. J. U. 1987. Prediction of HAZ Hardness of transformable Steels. *Metal Construction and British Welding Journal V* 119:217R-223R.

[65] Crossland, B. 1982. *Explosive welding of metals and its application*. *Oxford Series on Advanced Manufacturing*. Oxford: Clarendon Press.

[66] Song, J., A. Kostka, M. Veehmayer, and D. Raabe. Hierarchical microstructure of explosive joints: Example of titanium to steel cladding. *Materials Science and Engineering: A* 528 (6):2641-2647.

Table 1 – Chemical composition of the materials to be welded.

Composition- %wt	C	Si	P	S	Cr	Ni	Mn
AISI 304L	0.02	0.49	0.039	0.015	18.43	10.40	1.13
51CrV4	0.49	0.23	0.012	0.013	0.97	0.11	0.78

Table 2 – Weld series and density of explosives used.

Series	Explosive	Density (g/cm^3)
Weld 1	EEx+15% HGMB	0.774
Weld 2	EEx+11% HGMB	0.872
Weld 3	EEx+6% HGMB	0.923
Weld 4	EEx+2% EPS	0.733
Weld 5	EEx+1.5% EPS	0.820
Weld 6	ANFO	0.760

Table 3 – Calculated values of V_d, V_{pcal} and β, as well as the parameters used for the calculations.

Parameters	Weld reference					
	1	2	3	4	5	6
ΔH^*[kJ/kg]	3232	3232	3232	3232	3232	3880
C_0 [m/s]	4496	4496	4496	4496	4496	4496
$V_d = V_c$ [m/s]	3667	4000	4340	3233	3300	2370
P_{CJ} [GPa]	3.1	4.1	5.0	2.3	2.6	1.3
M/C [-]	0.51	0.45	0.43	0.54	0.48	0.52
T_{Vpcal} [μs]	2.3	2.3	2.3	2.3	2.3	2.3
V_{pcal} [m/s]	639	670	691	627	656	690
β [deg]	10.0	9.6	9.1	11.1	11.4	16.8

* ΔH is the heat of explosion. Values taken from Sanchidrián and Lopez [55].

Table 4 – Values of the parameters of equations (1) to (3) used for the calculation of the weldability window. All values taken from references [55; 56] unless stated otherwise.

Variable	Units	Equation	Value for the flyer plate	Value for the base plate
Re_{cr}; Reynolds Critical	[-]	1	10.5	
$H_{V,f}$; $H_{V,p}$- Vickers Hardness	[GPa] *	1, 2	1.491	1.912
ρ_f; ρ_p - Density	[kg/m^3] **	1 - 3	8030	7872
k1 – Empirical constant	[-]	2	0.6	
N – Empirical constant	[-]	3	0.11	-
T_m – Melting temperature	[^{o}C]	3	1454	-
C_0 – Bulk sound speed	[cm/s]	3	0.45x106 ***	-
C_p – Specific heat	[erg/g.^{o}C]	3	5.00x106	-
k – Thermal conductivity @500 ºC	[erg/m.^{o}C.s]	3	2.14x106	-
h – Flyer thickness	[cm]	3	0.15	-

*In Eq. (2) the hardness of the base plate is expressed in [N/m^2]. **In the Eq. (3) the density of the flyer plate is expressed in [g/cm^3]. ***[54].

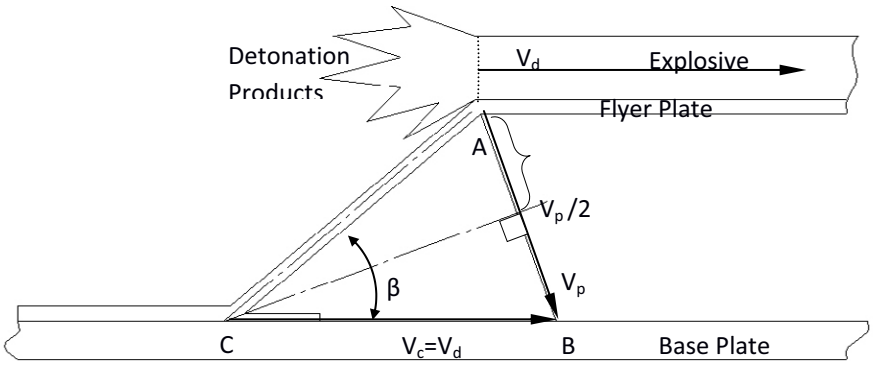

Fig

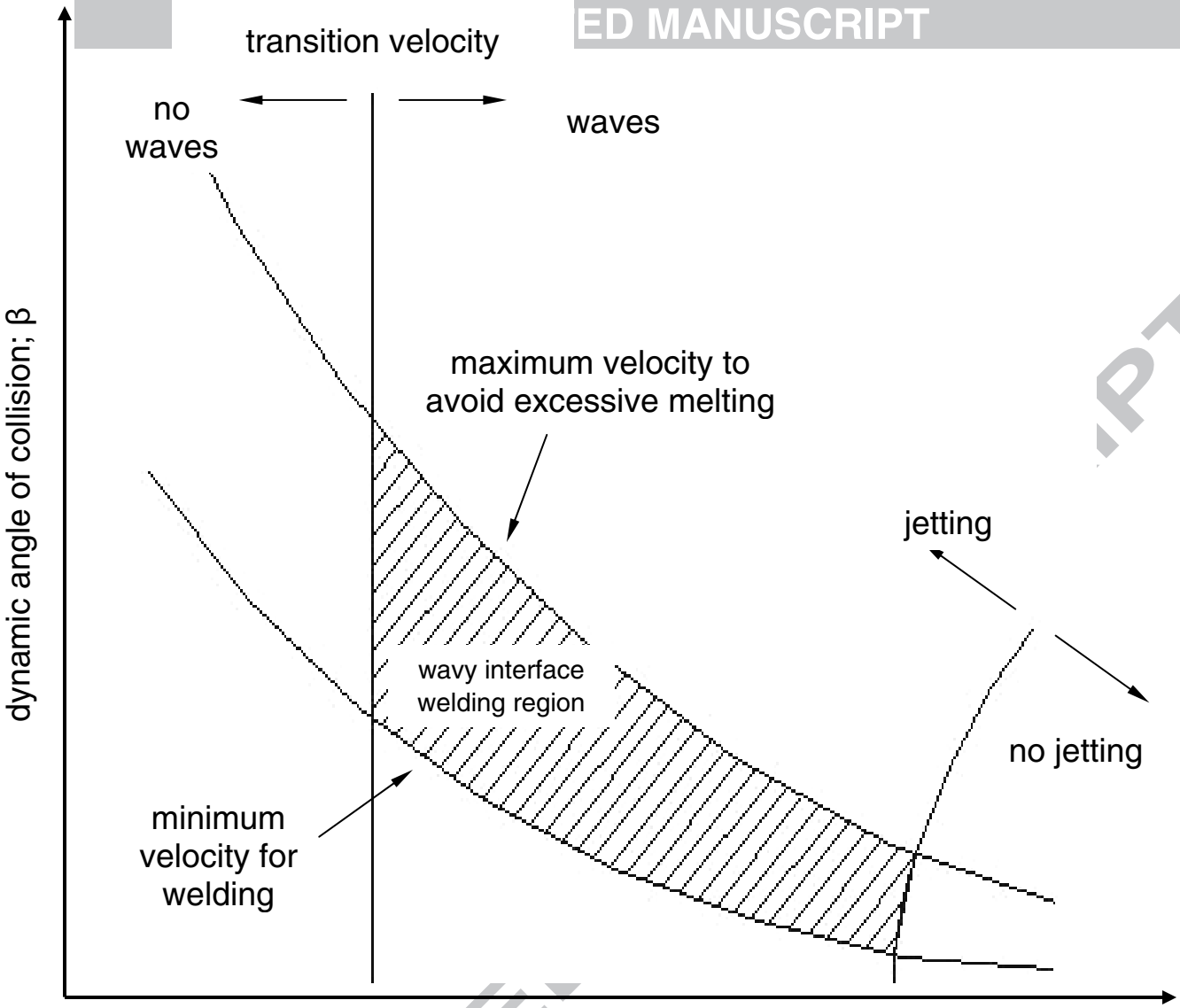

Fig 2

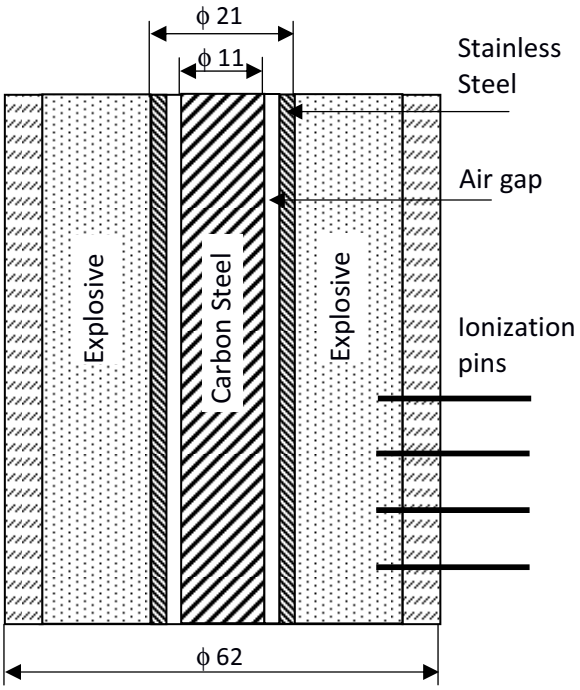

Fig 3

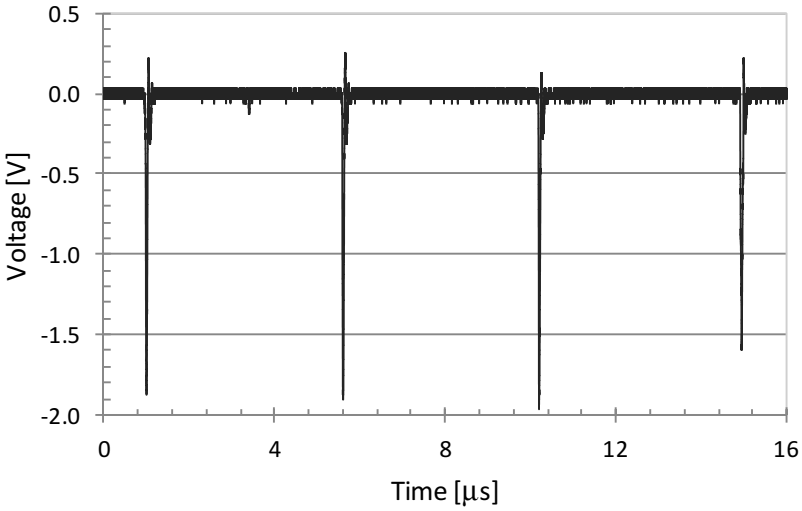

Fig 4

Fig 5

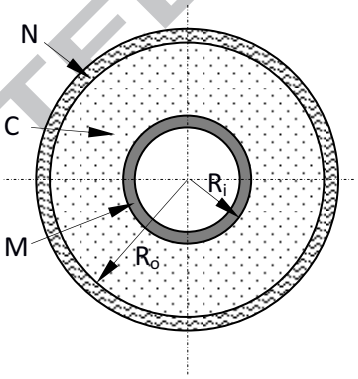

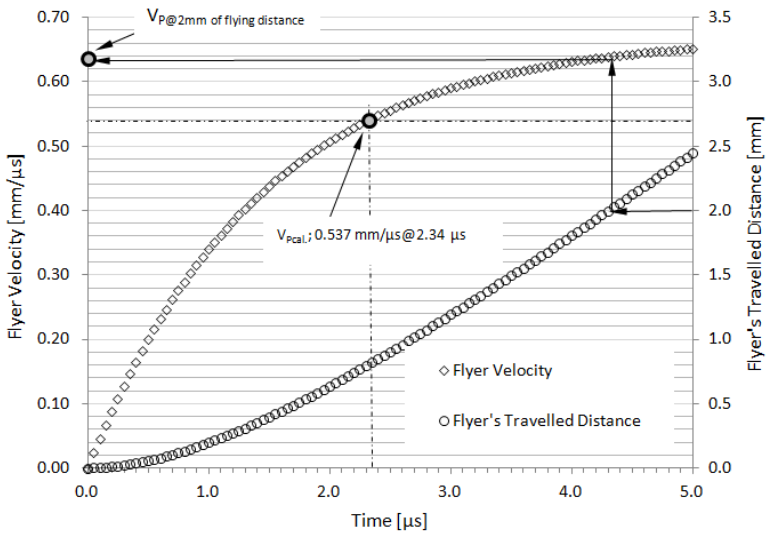

Fig 6

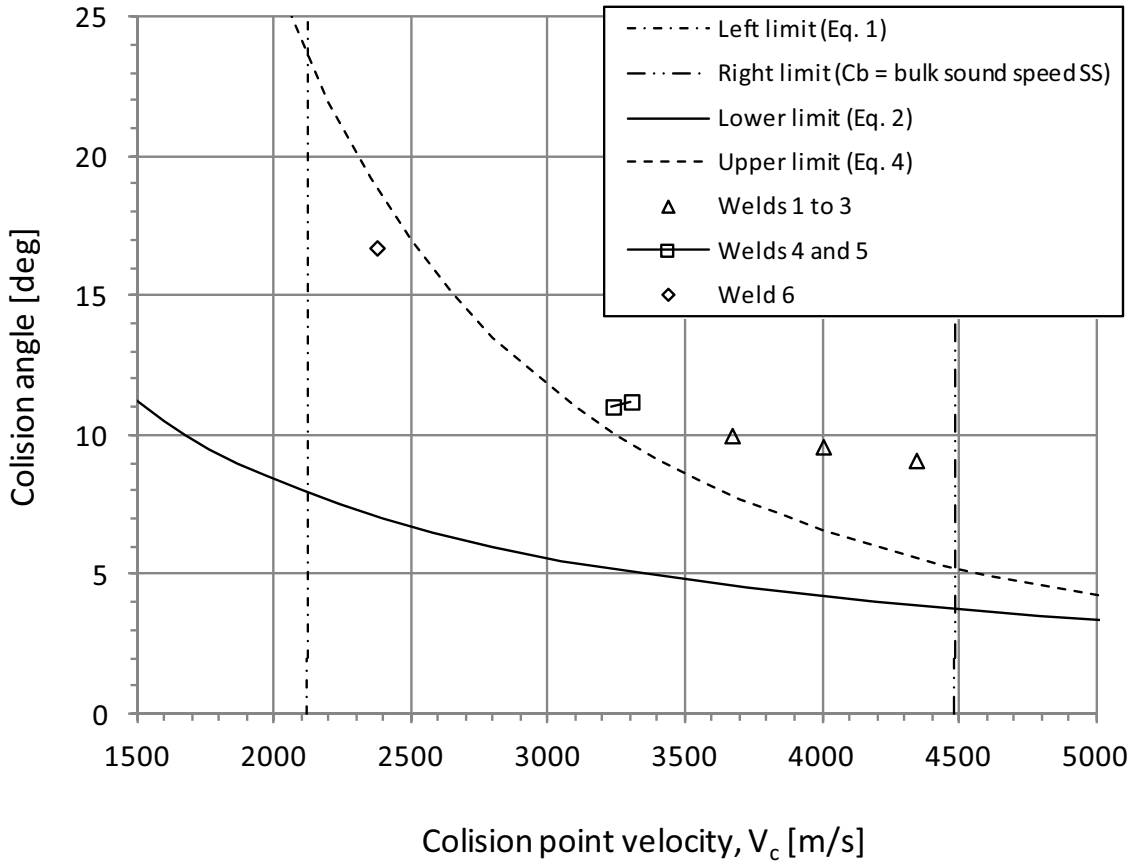

Fig 7

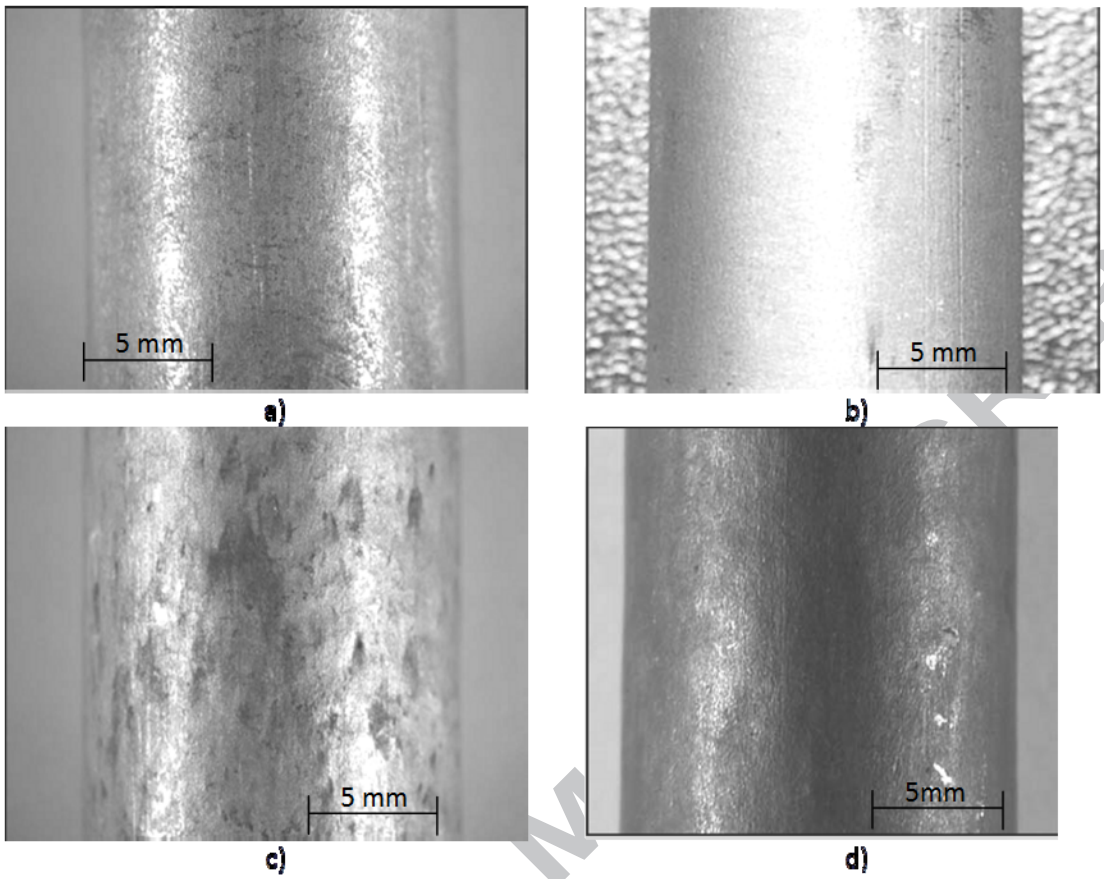

Fig 8

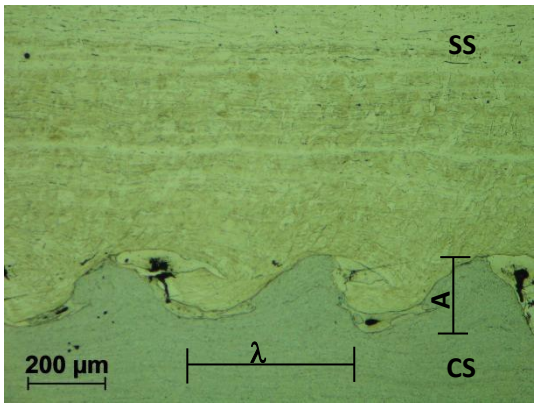

a) weld 1

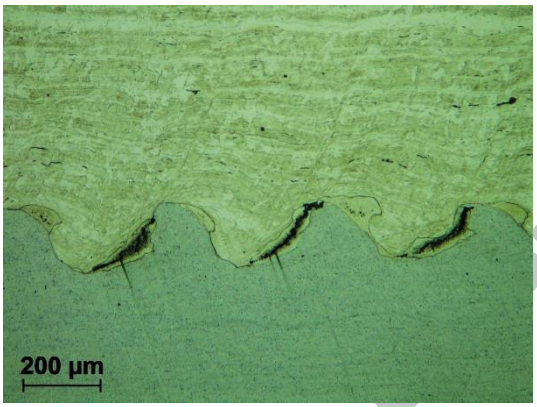

b) weld 2

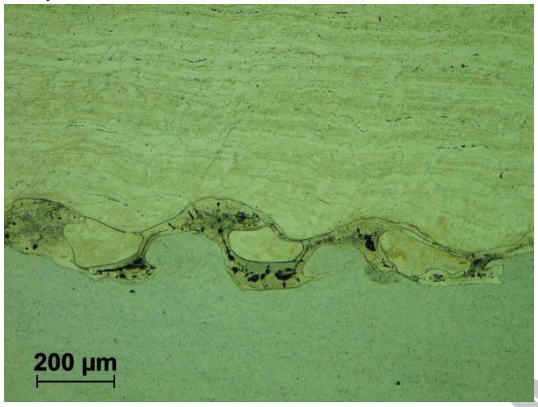

c) weld 3

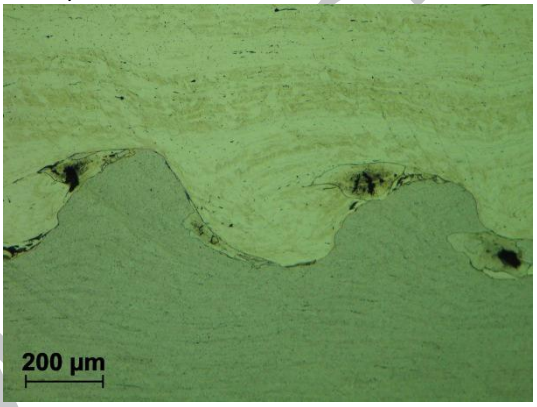

d) weld 4

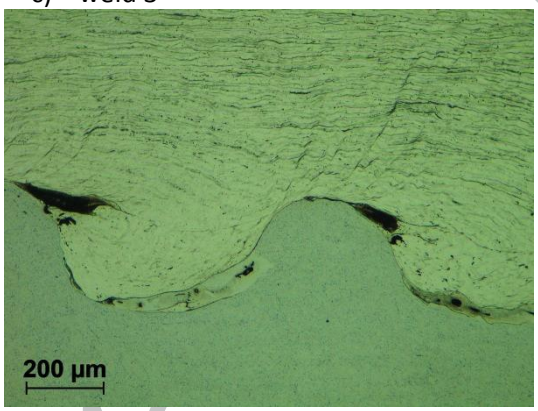

e) weld 5

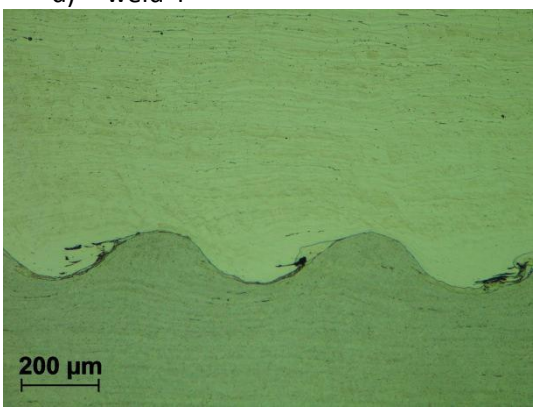

f) weld 6

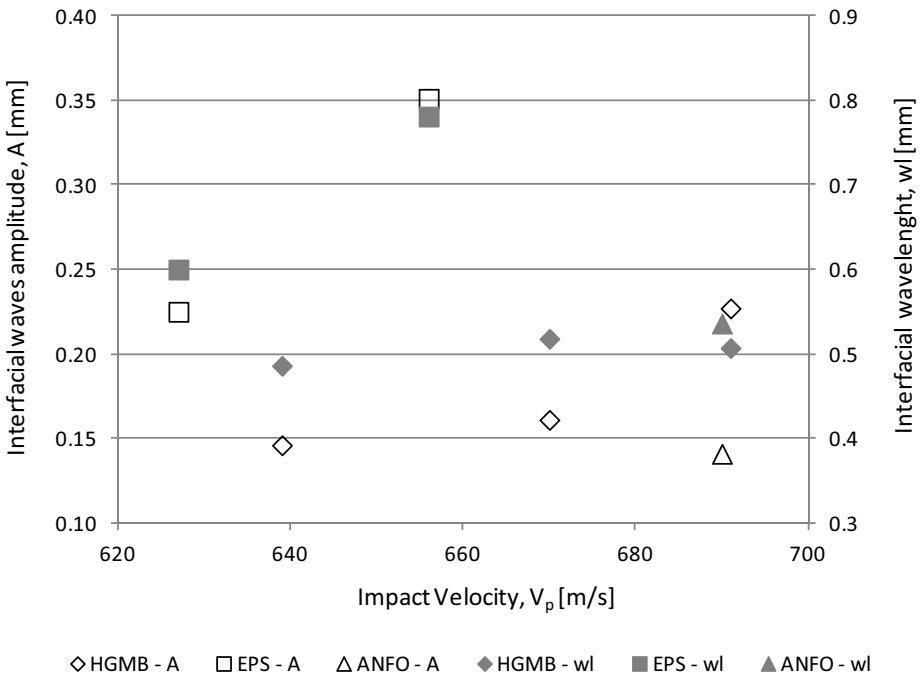

Fig 10

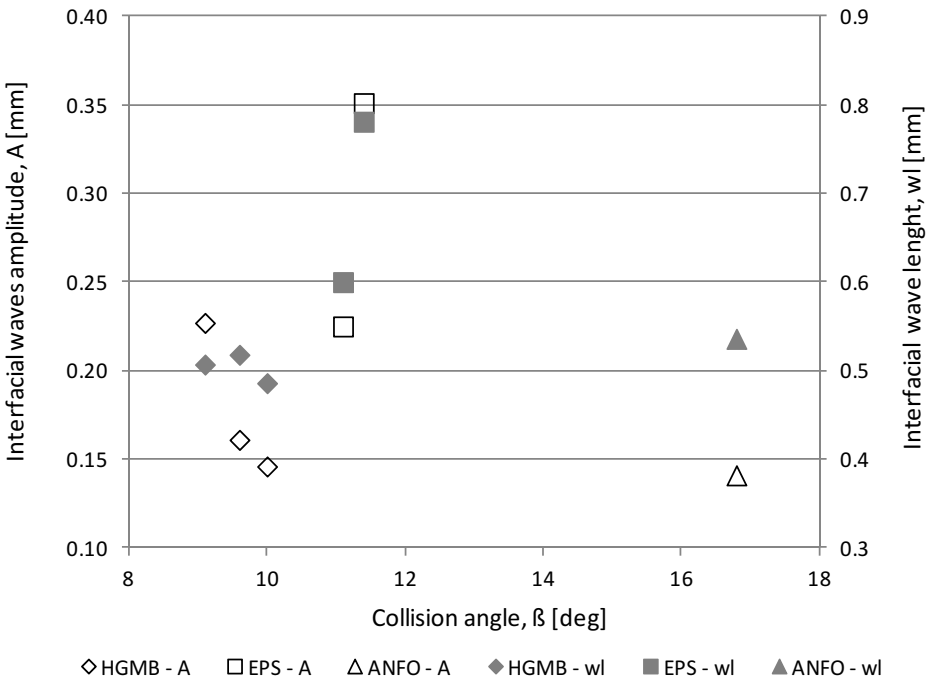

Fig 11

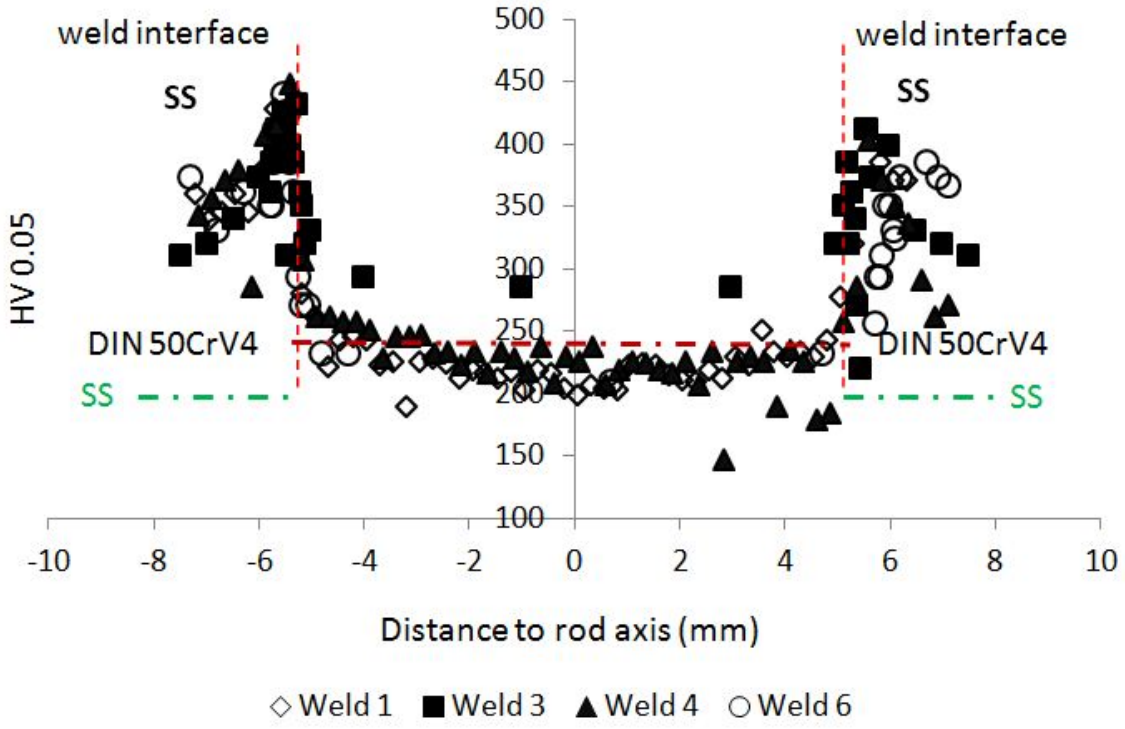

Fig 12

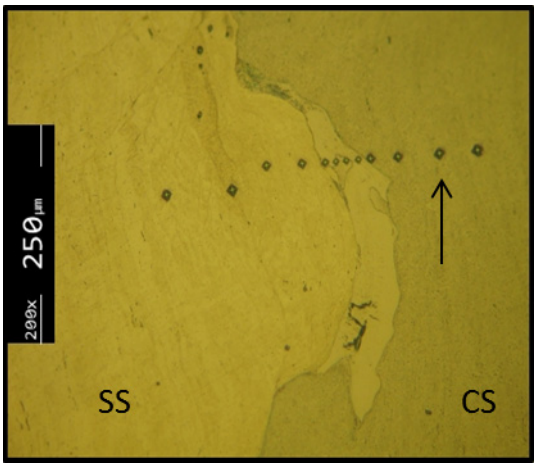

Fig 13

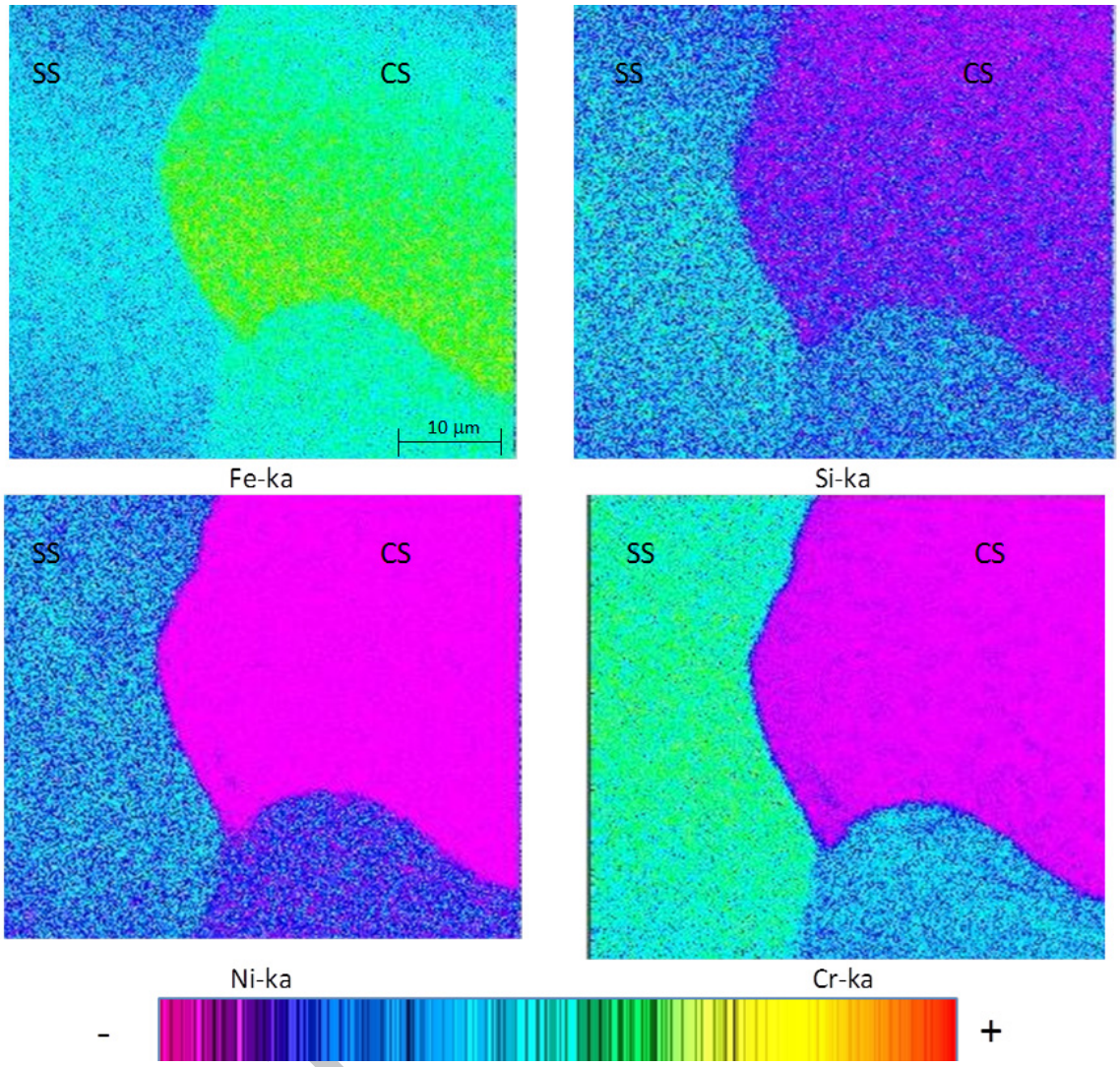

Fig 14

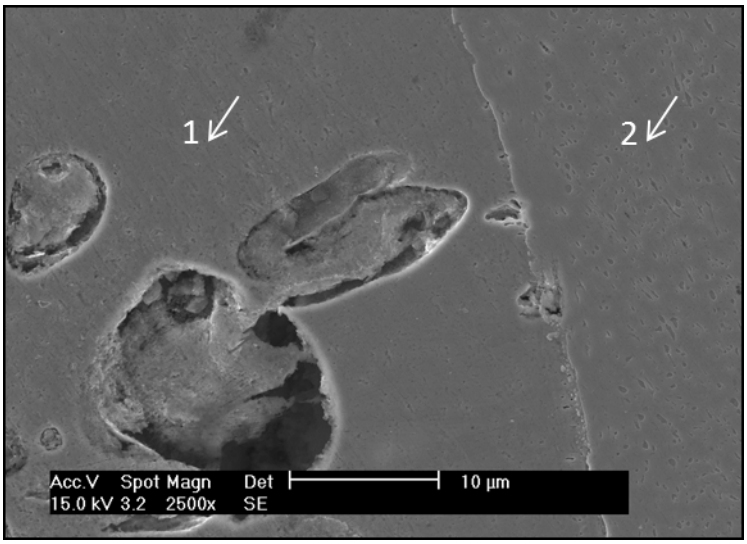

Fig 15

Explosive welding phenomena is detailed described and reviewed

The weldability window concept has shown to apply to cylindrical configuration

Evidence of Kelvin-Helmholtz mechanism on interfacial wave formation is shown

The Interfacial wavelength and amplitude are influenced by detonation stability